Available online at www.sciencedirect.com
ScienceDirect
Journal of Power Sources 162 (2006) 1172–1181
JOURNAL OF POWER SOURCES
www.elsevier.com/locate/jpowsour

Performance of Ni/ScSZ cermet anode modified by coating with $Gd_{0.2}Ce_{0.8}O_2$ for an SOFC running on methane fuel

Bo Huang *, X.F. Ye, S.R. Wang, H.W. Nie, J. Shi, Q. Hu, J.Q. Qian, X.F. Sun, T.L. Wen

Shanghai Institute of Ceramics, Chinese Academy of Sciences (SICCAS), 1295 Dingxi Road, Shanghai 200050, PR China

Received 19 June 2006; received in revised form 30 July 2006; accepted 31 July 2006
Available online 12 September 2006

Abstract

A Ni/scandia-stabilized zirconia (ScSZ) cermet anode was modified by coating with nano-sized gadolinium-doped ceria (GDC, $Gd_{0.2}Ce_{0.8}O_2$) prepared using a simple combustion process within the pores of the anode for a solid oxide fuel cell (SOFC) running on methane fuel. X-ray diffraction (XRD) and scanning electron microscopy (SEM) were employed in the anode characterizations. Then, the short-term stability for the cells with the Ni/ScSZ and 2.0 wt.%GDC-coated Ni/ScSZ anodes in 97%CH_4/3%H_2O at 700 °C was checked over a relative long period of operation. Open circuit voltages (OCVs) increased from 1.098 to 1.179 V, and power densities increased from 224 to 848 mW cm^{-2}, as the operating temperature of an SOFC with 2.0 wt.%GDC-coated Ni/ScSZ anode was increased from 700 to 850 °C in humidified methane. The coating of nano-sized $Gd_{0.2}Ce_{0.8}O_2$ particle within the pores of the porous Ni/ScSZ anode significantly improved the performance of anode supported cells. Electrochemical impedance spectra (EIS) illustrated that the cell with Ni/ScSZ anode exhibited far greater impedances than the cell with 2.0 wt.%GDC-coated Ni/ScSZ anode. Introduction of nano-sized GDC particles into the pores of porous Ni/ScSZ anode will result in a substantial increase in the ionic conductivity of the anode and increase the triple phase boundary region expanding the number of sites available for electrochemical activity. No significant degradation in performance has been observed after 84 h of cell testing when 2.0 wt.%GDC-coated Ni/ScSZ anode was exposed to 97%CH_4/3%H_2O at 700 °C. Very little carbon was detected on the anodes, suggesting that carbon deposition was limited during cell operation. Consequently, the GDC coating on the pores of anode made it possible to have good stability for long-term operation due to low carbon deposition.

Keywords: Solid oxide fuel cell (SOFC); Methane oxidation; Anode; Carbon deposition; Electrochemical impedance spectroscopy

1. Introduction

Solid oxide fuel cells (SOFCs) will inevitably exert a great impact on the development of the next generation energy technology and the hydrogen economy as fossil fuels are running out. At present, it has been launched into primeval stage of commercial manufacture in some developed countries. For conventional SOFCs, a high operating temperature (for example, 800–1000 °C) is required to ensure sufficiently high ionic conductivity and fast electrode kinetics, because of the low oxide ion conductivity of yttria-stabilized zirconia (YSZ) and the high overpotential at the electrode at lower operating temperature. However, the high operating temperature causes many serious problems such as: (1) severe restrictions on the choice of materials, (2) electrode sintering, (3) interfacial diffusion between electrode and electrolyte, and (4) mechanical stress due to different thermal expansion coefficient. To overcome these problems, it is desirable to operate SOFCs at reduced temperatures (≤800 °C). Reducing the operating temperature down to 600–800 °C brings both dramatic technical and economic benefits. The cost of SOFC technology may be dramatically reduced since much less expensive materials can be used in cell construction and novel fabrication techniques can be applied to the stack and system integration. Further, as the operating temperature is reduced, system reliability and operational life increase, as does the possibility of using SOFCs for a wide variety of applications, including residential and automotive applications [1–7]. In addition, SOFCs require hydrogen as the fuel, but viable near-term applications will need to use the more readily available hydrocarbons, such as methane. Therefore, much effort has

* Corresponding author. Tel.: +86 21 52411520; fax: +86 21 52413903.
E-mail address: huangbo2k@hotmail.com (B. Huang).

0378-7753/$ – see front matter © 2006 Elsevier B.V. All rights reserved.
doi:10.1016/j.jpowsour.2006.07.068

been devoted in developing reduced-temperature solid oxide fuel cells (SOFCs) running on hydrocarbon fuels instead of hydrogen [8–11]. However, conventional Ni-based anode suffers a number of drawbacks in systems where hydrocarbon fuel is used such as carbon deposition since Ni is a good catalyst for hydrocarbon cracking reaction. Carbon deposition covers the active sites of the anode, resulting in rapid, irreversible cell deactivation [12–16]. To minimize resistive loss across the electrolyte membrane, many researchers have developed anode-supported SOFCs based on a thin-film electrolyte [17–19]. The electrode overpotentials and carbon deposition have remained major problems for reduced-temperature SOFCs running on hydrocarbon fuels.

In this study, a novel Ni/scandia-stabilized zirconia (ScSZ) cermet anode was prepared by coating $Gd_{0.2}Ce_{0.8}O_2$ (GDC) nanometer grains within the pores of porous Ni/ScSZ anode using an auto-ignited combustion process with a citrate-metal nitrate precursor. Yoon et al. [20] have demonstrated that the YSZ or SDC layers deposited within the cathode can provide paths for oxide ions and expand the reaction zone into the new triple phase boundary (TPB). In addition, ceria is known to readily store and transfer oxygen, and adding zirconia enhances the storage capability [21]. The present work aimed to study the effect of the $Gd_{0.2}Ce_{0.8}O_2$ coating on the Ni/ScSZ anode using electrochemical impedance spectroscopy (EIS) and dc polarization methods. The results clearly show that the coating of nanometer grains $Gd_{0.2}Ce_{0.8}O_2$ within the pores of porous Ni/ScSZ anode not only improves the kinetics of hydrogen or methane oxidation reaction but also significantly reduces the degradation in performance of the Ni/ScSZ anode in humidified methane.

2. Experimental

2.1. Starting materials

The material system used in this work was based on commercial nickel oxide (NiO, Inco Canada) powder and scandia-stabilized zirconia $Zr_{0.89}Sc_{0.1}Ce_{0.01}O_{2-x}$ (ScSZ, Daiichi Kigenso Kagaku Kogyo, Japan) powder, solvent, dispersant, binder, plasticizer and pore formers. The solvent system used in this paper consisted of azeotropic mixture of butanone and ethyl alcohol absolute in order to avoid differential evaporation. Triethanolamine as a kind of zwitterionic dispersant was used as dispersant. Poly-vinyl-butyl (PVB) and polyethylene glycol (PEG 200) were used as binder and plasticizers, respectively. The PVB binder was supplied as a free flowing fine-grained powder and the PEG plasticizer was obtained in a liquid form. Ammonium oxalate as pore formers was added to the anodic mixture in order to increase porosity. All the organic additives were supplied by Shanghai Chem. Ltd., China.

2.2. Preparation of Ni/ScSZ powder and the anode matrix

The anode matrix of Ni/ScSZ was produced by tape casting NiO and ScSZ slurry containing ammonium oxalate pore formers, followed by sintering at 1450 °C for 2 h. The slurries for the tape casting process were fabricated by a ball milling method that included three steps. Firstly, in order to prepare suitable anode powders for anode-supported type cells, Ni/ScSZ anode matrix was made by adding 100 g NiO powder and ScSZ powder in a weight ratio of 1:1 to 1 g dispersant. The ingredients were mixed thoroughly with 80 g butanone/ethyl alcohol absolute solvents and the slurry was ball milled for 2 h in order to break weak agglomerates. Secondly, 10 g PVB and 10 g PEG were added to the above system and the resulting slurry was ball milled for an additional 2 h. In the third step, 20 g ammonium oxalate pore formers (200 mesh) was then added to the mixture and the ball milling was continued for 0.5 h. After the mixing and the homogenization of the slurry were completed, the slurry was degassed using a vacuum pump (pressure: 200 mbar absolute) and cast on a casting surface of polyethylene film by a "doctor-blade" method. The cast tapes were allowed to dry at room temperature for 48 h. After the solvent in the tapes was completely evaporated, the Ni/ScSZ green tapes were obtained. They were then sintered in the air at 1450 °C for 2 h. The porosities of the sintered Ni/ScSZ layers were determined using either Hg porosimetry (Pore Sizer 9320) or a standard test method based on Archimedes' principle by measuring the mass of water that could be absorbed into the Ni/ScSZ layer [22]. Thus, a disk-shaped anode substrate, or a fuel electrode, having a diameter of about 3.0 cm, a thickness of 1 mm, and a porosity of about 42%, was then produced. Scanning electron microscope (SEM) images of the sintered Ni/ScSZ layer before and after SOFC single cell operation were analyzed using a microscope (SEM, PHILIPS 515, Holland) equipped with an X-ray analyzer for energy-dispersive X-ray spectroscopy (EDS).

2.3. Fabrication of unit-cells

Ni/ScSZ anode-supported SOFCs were fabricated using a dual tape cast layers of Ni/ScSZ and ScSZ, one containing pore formers (the porous Ni/ScSZ anode matrix) and one without pore formers (the ScSZ electrolyte layer). The electrolyte layer was cast first and then allowed to dry at room temperature for 48 h. A second layer of Ni/ScSZ which contained pore formers was then cast on top of the electrolyte green tape and allowed to dry overnight. The composite structure was then co-sintered in the air at 1450 °C for 2 h. The green layers of cathodes with $\pi(0.7\,\text{cm})^2 = 1.5386\,\text{cm}^2$ area were fabricated by screen-printing a slurry containing $(Pr_{0.7}Ca_{0.3})_{0.9}MnO_3$ onto the surface of the dense ScSZ electrolyte and then sintering at 1200 °C for 2 h. SEM images showed that the thickness of electrolyte and cathode of the single cell was 15 and 20 μm, respectively.

2.4. $Gd_{0.2}Ce_{0.8}O_2$ coating

$Gd_{0.2}Ce_{0.8}O_2$ precursor gel was prepared as follows. Initially, stoichiometric amounts of gadolinium nitrate ($Gd(NO_3)_3{\cdot}6H_2O$) and cerium nitrate ($Ce(NO_3)_3{\cdot}6H_2O$) were dissolved in distilled water with constant stirring. Then, a stoichiometric amount of citric acid ($C_6H_8O_7{\cdot}H_2O$), which is a chelating agent and fuel, was also dissolved in this solution.

The stoichiometric ratio of citric acid to nitrates was calculated according to Jain et al. [23]. The Ce^{3+} concentration in the transparent solution was 4 mol dm^{-3}. The solution pH was maintained between 7 and 8. The porous anode layer Ni/ScSZ of anode-supported cell was completely dipped in the above solution and evacuated using a vacuum pump set to an absolute pressure of 200 mbar for 10 min, so that the solution filled the pores of the Ni/ScSZ layer. Then, it was dried at 75 °C, followed by calcination at 600 °C for 2 h. This procedure was repeated several times to have a uniform coating. The impregnated $Gd_{0.2}Ce_{0.8}O_2$ loading in Ni/ScSZ anode was estimated from the weight change of the anode coating before and after the impregnation treatment. The impregnated GDC loading was about 2.0 wt.% after two GDC impregnation treatments.

2.5. Characterization of anode performance and single cell performance

SOFC tests were carried out in a single cell test setup which was basically similar to that proposed by Zheng et al. [24]. A Pt mesh and lead wire were attached to the surface of the cathode using a Pt ink, followed by sintered at 950 °C for 0.5 h. On the anode side, a Au mesh and lead wire were used as the current collector and were attached using a Au ink applied to the edges of the Au mesh, followed by sintering at 850 °C for 0.5 h. The anode side of the structure was then attached to an alumina tube using Au ink and the edges were sealed using a ceramic adhesive. All the anodes were evaluated with the same testing procedure. The anodes were fully reduced in H_2 atmosphere at 850 °C for 0.5 h prior to cell testing. Hydrogen and methane humidified at room temperature (~3%H_2O) were used as fuel and oxygen was used as oxidant. The fuel and oxidant flow rate were all controlled at 25 sccm. The current–voltage curves and electrochemical impedance spectroscopy (EIS) were obtained using an Electrochemical Workstation IM6e (Zahner, GmbH, Germany). These measurements were started after stabilizing under a constant discharge voltage of 0.7 V for 4 h, in order to obtain a sufficiently stabilized system necessary for a cell testing experiment. Then, the current was switched off and the impedance spectra of the electrochemical cell were recorded under open circuit from time to time for 84 h with amplitude of 10 mV over the frequency range 0.02 Hz to 100 kHz. The measurement was carried out in the temperature range of 700–850 °C in steps of 50 °C. The ohmic resistance of the electrolyte, the cathode and the anode ($R\,\Omega$)was estimated from the high frequency intercept of the impedance curves and the overall electrode polarization (interface) resistance (R_E) was directly measured from the differences between the low and high frequency intercepts on the impedance curves.

3. Results and discussion

3.1. Microstructural characterization

3.1.1. XRD characterization

Fig. 1 shows the X-ray diffraction patterns of $Gd_{0.2}Ce_{0.8}O_2$ powders obtained from the gel after heat treatment at different temperatures ranging between 500 and 900 °C. It is clearly seen that the compound formation starts at 500 °C and crystalline product could be obtained at 600 °C. From the TEM image of the synthesized powder as shown in Fig. 2, $Gd_{0.2}Ce_{0.8}O_2$ grains with nanometer size could be clearly observed. The $Gd_{0.2}Ce_{0.8}O_2$ formation onto the Ni/ScSZ anode was confirmed by matching the individual peaks. Fig. 3 shows the XRD pattern of $Gd_{0.2}Ce_{0.8}O_2$ coated Ni/ScSZ anode sintered at 600 °C. Individual peaks corresponding to $Gd_{0.2}Ce_{0.8}O_2$, NiO and ScSZ are marked in the figure. From the above analysis, it can be inferred that the ultra fine $Gd_{0.2}Ce_{0.8}O_2$ grains may coat the surface of the porous Ni/ScSZ anode by burning the citrate + nitrate solution that filled the pores and covered the surface of the porous Ni/ScSZ anode.

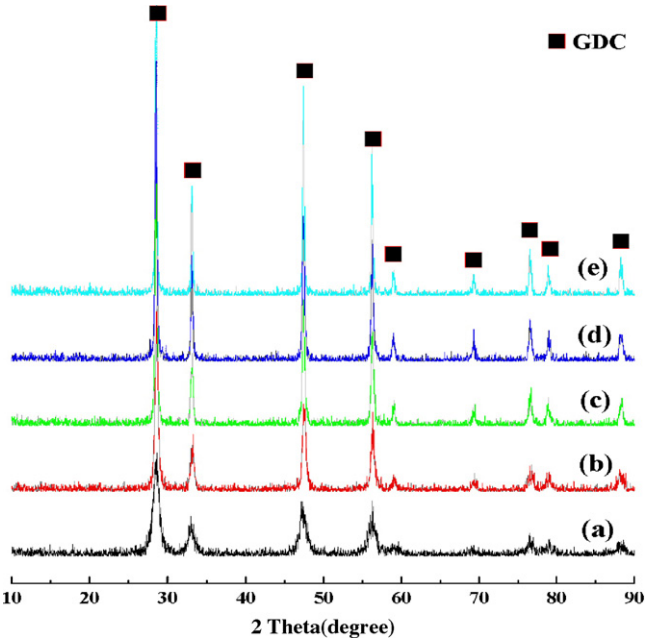

Fig. 1. X-ray diffraction patterns of $Gd_{0.2}Ce_{0.8}O_2$ obtained after different heat treatment of the gel precursor: (a) 500 °C, (b) 600 °C, (c) 700 °C, (d) 800 °C and (e) 900 °C.

3.1.2. SEM characterization

Fig. 4 shows the cross-sectional SEM micrographs of the Ni/ScSZ anode and the 2.0 wt.%GDC-coated Ni/ScSZ anode,

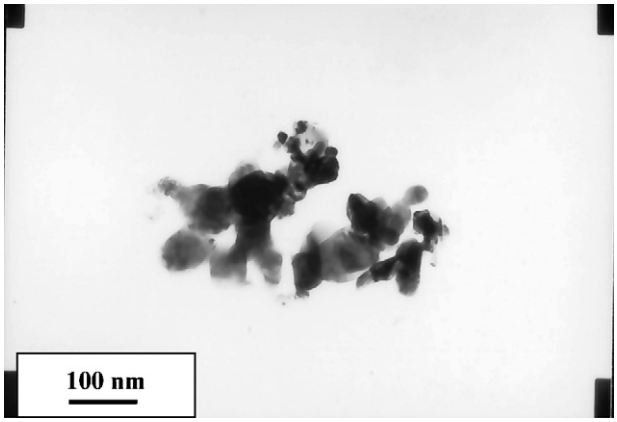

Fig. 2. TEM image of combustion-synthesized $Gd_{0.2}Ce_{0.8}O_2$ powder calcined at 600 °C for 2 h.

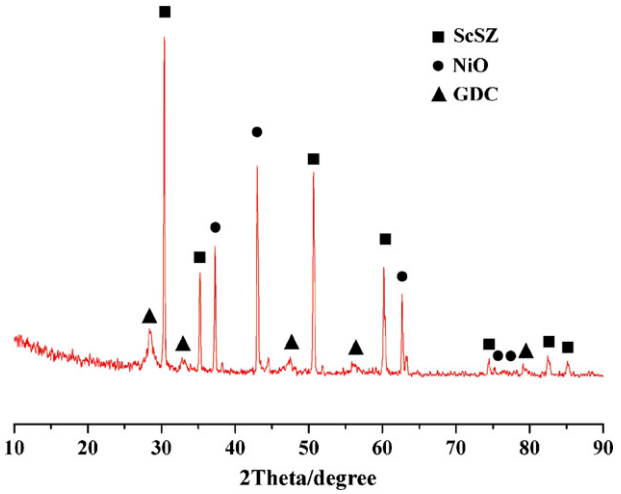

Fig. 3. X-ray diffraction patterns of $Gd_{0.2}Ce_{0.8}O_2$ coated porous Ni/ScSZ anode sintered at 600 °C.

respectively. The morphological difference between Ni/ScSZ and 2.0 wt.%GDC-coated Ni/ScSZ anode could be attributed to the $Gd_{0.2}Ce_{0.8}O_2$ coating within the pores of porous Ni/ScSZ anode followed by sintering. The 2.0 wt.%GDC-coated Ni/ScSZ anode had a good pore structure. In comparison with the cross-sectional SEM micrographs of Ni/ScSZ, the counterparts of the pre-treated Ni/ScSZ were covered with many tiny GDC grains, which were tightly sintered with the Ni/ScSZ.

3.2. Current–voltage measurements

Figs. 5 and 6 show typical voltage and power density versus current density of an SOFC with Ni/ScSZ and 2.0 wt.%GDC-coated Ni/ScSZ anodes while operating on humidified hydrogen (a) and methane (b), respectively. The data show a significant increase in performance as the nano-sized $Gd_{0.2}Ce_{0.8}O_2$ grains coated the surface of the porous Ni/ScSZ anode while running on humidified hydrogen and methane. The performance of the cell with Ni/ScSZ anode while operating on humidified hydrogen

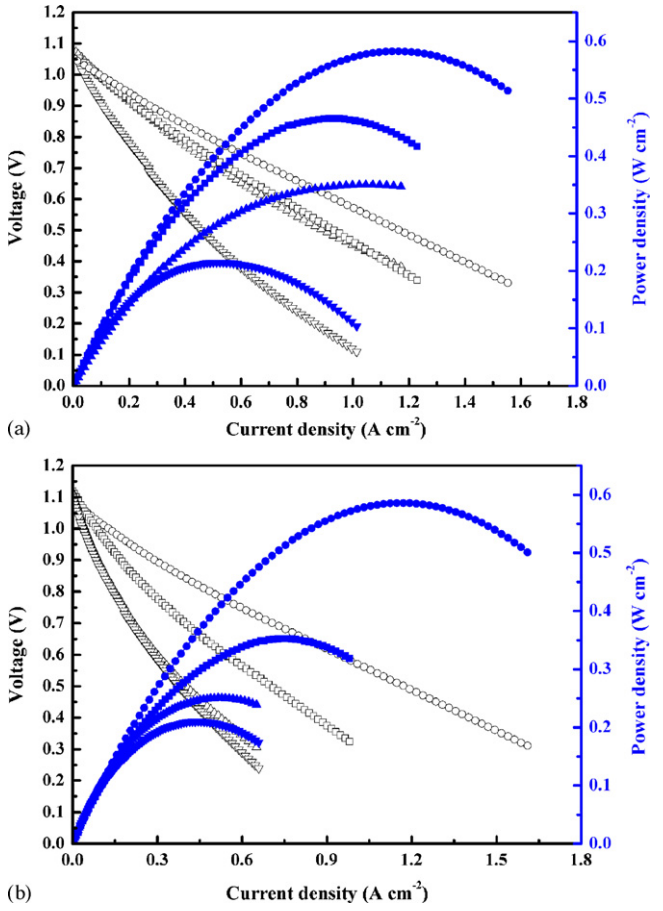

Fig. 5. Voltage and power density vs. current density for an SOFC with Ni/ScSZ anode while running on humidified hydrogen (a) and methane (b) at different temperatures: (◯, ●) 850 °C; (□, ■) 800 °C; (▲, △) 750 °C; (▼, ▽) 700 °C.

was modest with a maximum power density of 584, 466, 345 and 212 mW cm^{-2} at 850, 800, 750 and 700 °C, respectively, and whereas the corresponding values were 825, 602, 398 and 238 mW cm^{-2} for the cell with 2.0 wt.%GDC-coated Ni/ScSZ anode. The highest power density of the cell with Ni/ScSZ anode

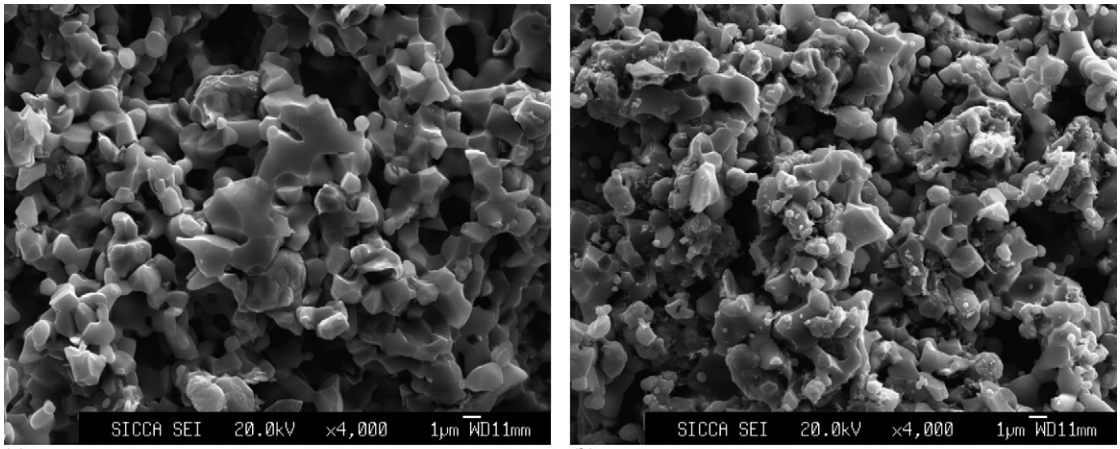

Fig. 4. SEM cross-sectional micrographs of (a) Ni/ScSZ anode and (b) 2.0 wt.%GDC-coated Ni/ScSZ anode.

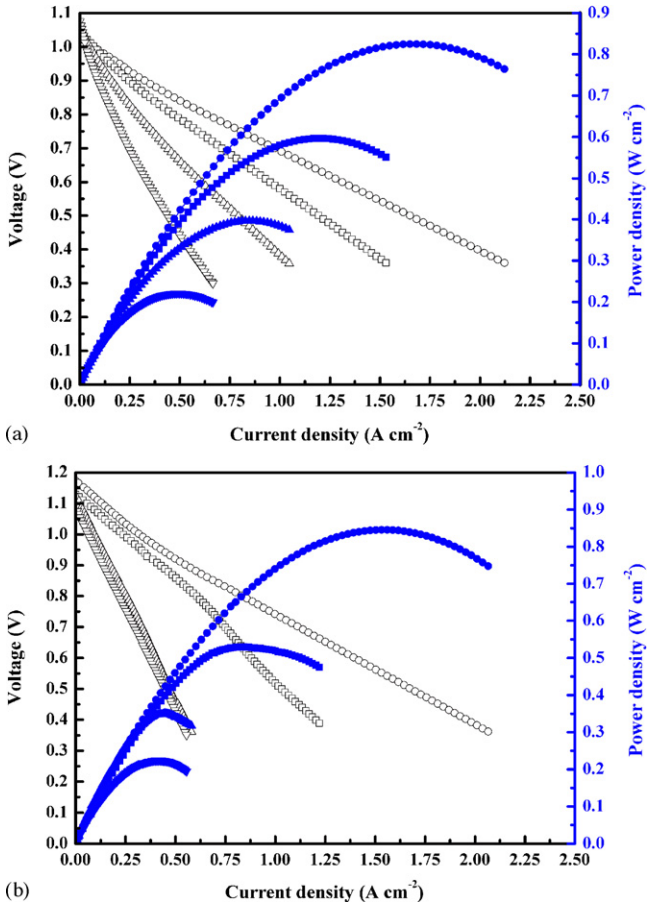

Fig. 6. Voltage and power density vs. current density for an SOFC with 2.0 wt.%GDC-coated Ni/ScSZ anode while running on humidified hydrogen (a) and methane (b) at different temperature for 48 h: (◯, ●) 850 °C; (□, ■) 800 °C; (▲, △) 750 °C; (▼, ▽) 700 °C.

while operating on humidified methane was 586, 352, 251 and 205 mW cm^{-2} at 850, 800, 750 and 700 °C, respectively. The counterpart of the cell with 2.0 wt.%GDC-coated Ni/ScSZ anode while operating on humidified methane was 848, 529, 350 and 224 mW cm^{-2} at 850, 800, 750 and 700 °C, respectively.

The *I–V* curves showed positive curvature, particularly at lower temperatures. This is similar to reports on anode-supported cells operating on hydrogen [25,26]. A detailed study of anode-supported cells running on hydrogen has shown that cell power densities can be limited by a number of factors, including concentration polarization [26]. The decrease in cell power density for methane relative to hydrogen may be related to the higher mass of methane molecules, which yields slower gas-phase diffusion and increased concentration polarization. However, it is also noted that each methane molecule reacts with four times as many oxygen ions as each hydrogen molecule, so less methane gas-phase diffusion is needed to yield the same cell current density. Another possible explanation is a difference in the nature of the oxidizing and reducing species, which makes the charge transfer in methane more complex and difficult. H_2 is obviously more active and more effective for reduction. CH_4 is much less reactive than H_2 in heterogeneous oxidation [27], thus resulting in a higher polarization resistance associated with slower electrochemical oxidation of methane versus hydrogen.

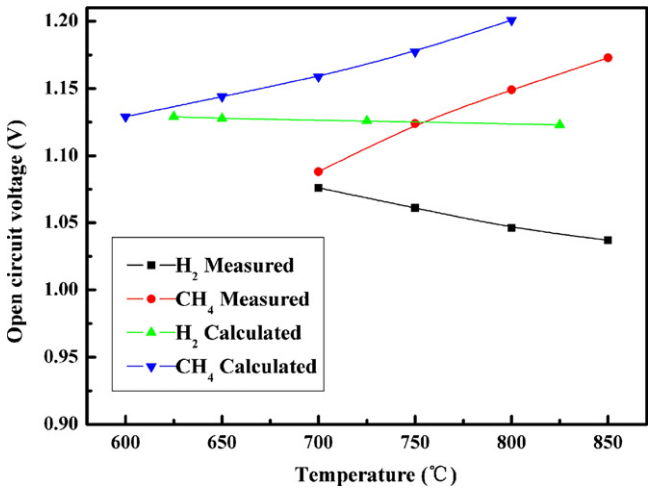

Fig. 7. Open circuit voltage values vs. temperature for both hydrogen and methane. Also shown are the values predicted by assuming that the humidified methane reaches an equilibrium composition.

Measured open circuit voltage (OCV) values for an SOFC with 2.0 wt.%GDC-coated Ni/ScSZ anode are plotted versus temperature for both hydrogen and methane in Fig. 7. OCV values were measured immediately after stable cell operation at 0.7 V. The OCV values for methane increased linearly with increasing temperature, opposite of the trend shown for hydrogen. The OCV values at high temperatures are in agreement with Liu and Barnett's results [28]. The OCV values of 1.098 ~ 1.179 V for an SOFC with 2.0 wt.%GDC-coated Ni/ScSZ anode measured at 700 ~ 850 °C is between the values measured at 1000 °C, 1.2 V, and at 550 ~ 650 °C, 1.05 V [28]. Also shown in Fig. 7 are the predicted OCV values, assuming that the humidified methane reaches equilibrium. The experimental OCV values are fundamentally in agreement with the predicted ones, although the experimental values are about 40 mV lower. Experimental OCV values are typically slightly less than theoretical, presumably indicating slight gas leaks in the single cell test.

3.3. Electrochemical impedance spectroscopy (EIS) study

Figs. 8 and 9 show a comparison of typical EIS results, from cells with Ni/ScSZ anode and 2.0 wt.%GDC-coated Ni/ScSZ anode operated in humidified hydrogen and methane under open circuit at different temperature, respectively, associated with the *V–I* curves in Figs. 5 and 6. As could be expected through examination of Figs. 8 and 9, the cell with 2.0 wt.%GDC-coated Ni/ScSZ anode exhibits far less total impedance than that observed for the cell with Ni/ScSZ anode. The rapid electrochemical oxidation of hydrogen or methane at these temperatures was due to the anodes employed in these SOFCs, which combined Ni/ScSZ and nano-sized GDC particles. Impedance measurements taken in humidified hydrogen or methane for Ni/ScSZ and 2.0 wt.%GDC-coated Ni/ScSZ anodes indicate that the nano-sized GDC particles caused the interfacial resistance

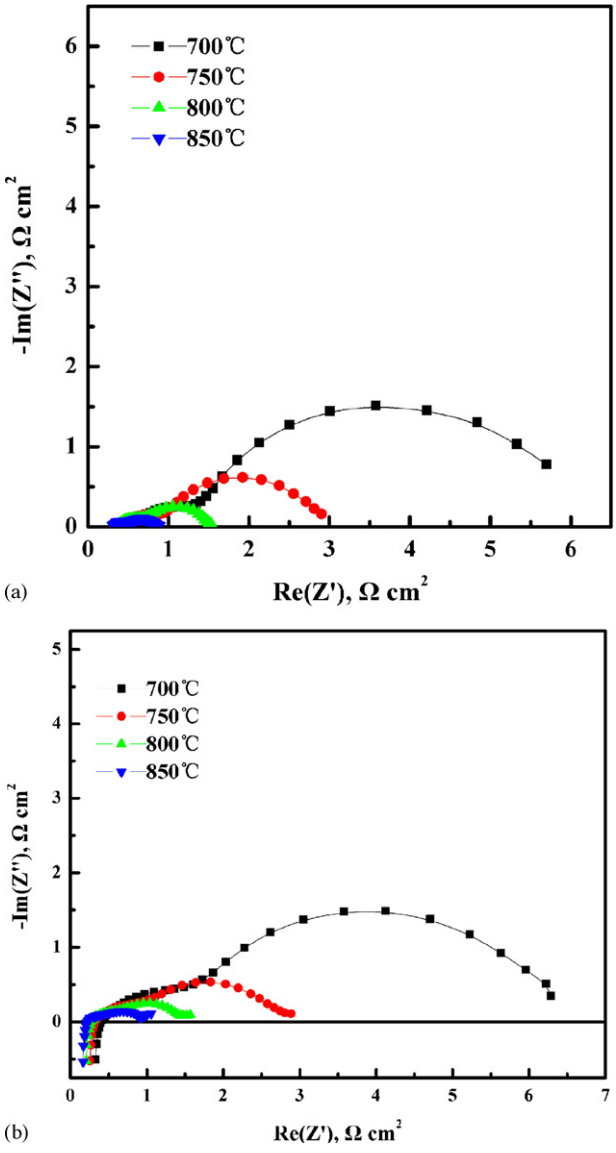

Fig. 8. Electrochemical impedance spectra for an SOFC with Ni/ScSZ anode while running on humidified hydrogen (a) and methane (b) at different temperature under open circuit.

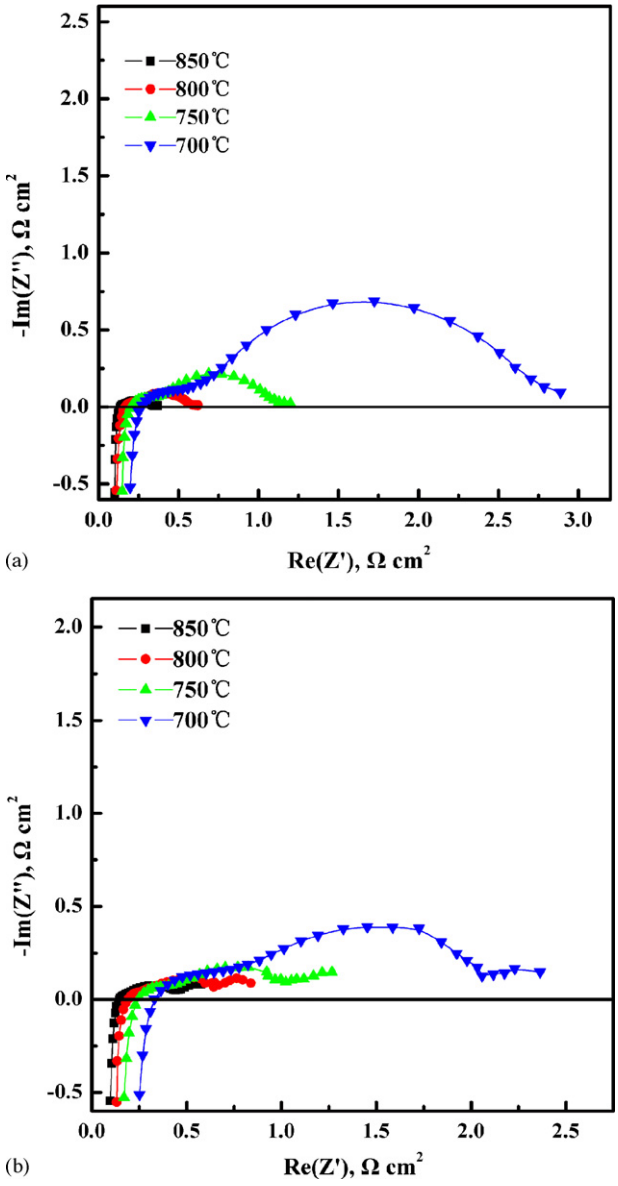

Fig. 9. Electrochemical impedance spectra for an SOFC with 2.0 wt.%GDC-coated Ni/ScSZ anode while running on humidified hydrogen (a) and methane (b) at different temperature under open circuit.

to reduce by a factor of ∼2. It is well known that gadolinium-doped ceria is beneficial for several reasons. First, it becomes a mixed conductor in the reducing atmosphere [29], a condition which should expand the reaction zone beyond three-phase boundaries. Second, the ionic conductivity of gadolinium-doped ceria is higher than that of ScSZ, which improves the transport of oxygen ions from the electrolyte to the anode. Third, gadolinium-doped ceria is known to readily store and transfer oxygen, and adding zirconia enhances the storage capability [30]. The present anodes have additional ceria/zirconia interfaces where enhanced oxygen storage may increase hydrogen or methane oxidation rates. Therefore, introduction of gadolinium-doped ceria into the pores of porous Ni/ScSZ anode will result in a substantial increase in the ionic conductivity of the anode and increase the triple phase boundary region expanding the number of sites available for electrochemical activity.

3.4. Cell stability tests

The stabilization and the degradation of the two cells with Ni/ScSZ and 2.0 wt.%GDC-coated Ni/ScSZ anodes were also investigated in 97%CH_4/3%H_2O at 700 °C during the measurements. The electrochemical impedance spectra were measured during the aging process. Fig. 10 depicts the electrochemical impedance spectra for the two cells with Ni/ScSZ and 2.0 wt.%GDC-coated Ni/ScSZ anodes at 700 °C under open circuit at different operating time. As can be seen from Fig. 10, the overall electrode polarization (interface) resistance (R_E) is decreasing sharply with time initially. This implies that, in the case of two anode materials, the electrochemical reaction rates are increasing rapidly with time. Then, R_E increases gradually with time suggesting that the corresponding electrochem-

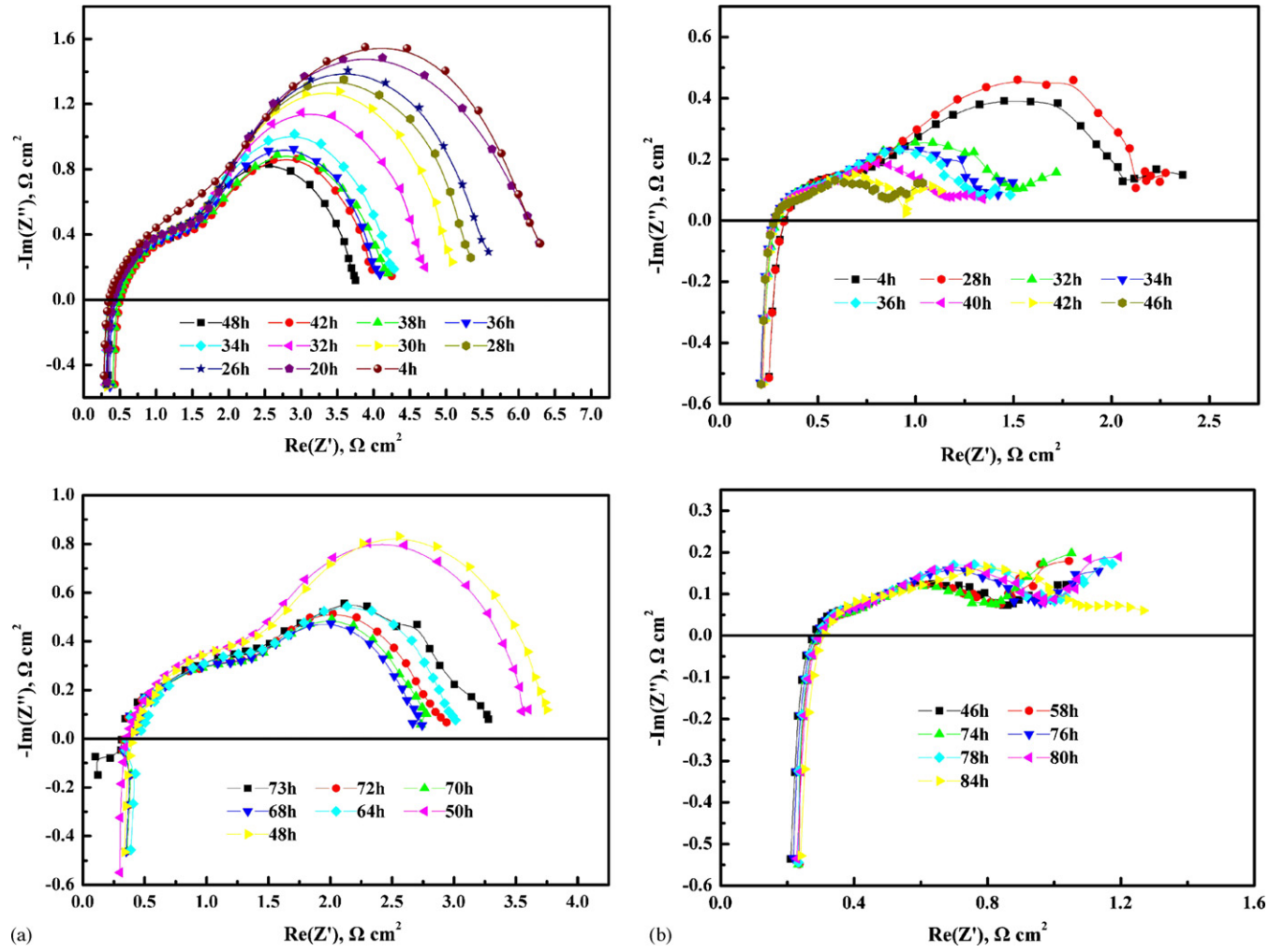

Fig. 10. Electrochemical impedance spectra of (a) Ni/ScSZ anode and (b) 2 wt.%GDC-coated Ni/ScSZ anode in 97%CH_4/3%H_2O at 700 °C under open circuit during the aging process.

ical reaction rates are decreasing slowly with time (in terms of Ni/ScSZ, 2.0 wt.%GDC-coated Ni/ScSZ, after 68 and 74 h, respectively). The variation of the overall electrode polarization resistance with time for the two cells with Ni/ScSZ and 2.0 wt.%GDC-coated Ni/ScSZ anodes indicates that the electrochemical oxidation reaction of CH_4 are not taking place under constant conditions, rather the conditions at the anode surface are modified with the time of exposure to 97%CH_4/3%H_2O. These surface modifications affect electrochemical performance of anode samples. The changes in the impedance spectra can be assumed to be due to carbon deposition in the anode, which happened after operation of 20 and 28 h in terms of Ni/ScSZ and 2.0 wt.%GDC-coated Ni/ScSZ, respectively. Visual inspection of the cell after the end of the test revealed carbon deposition on the anode material and the surroundings. The decrease of R_E after carbon deposition can be understood by a model similar to that proposed by Gorte and co-workers [31]. Metal Ni in the anode acts also for the efficient current collection. Some metal Ni particles are expected to be not connected to the outside circuit and cannot assist in the removal of electrons. Therefore, the entire region under the isolated metal Ni particle is ineffective for the electrochemical reaction. With the addition of moderate levels of carbon, these isolate metal Ni particles could become electronically connected to the outside circuit. Because more of the anode surface is now involved in the electrochemical reaction, the effect of using a higher fraction of the surface will be an apparent decrease in polarization resistances. With the addition of a certain levels of carbon, deposited carbon began to cover the active sites of the anode and block the pores of gas diffusion, resulting in an increase in polarization resistances. In one case, a cell with 2.0 wt.%GDC-coated Ni/ScSZ anode was operated for >84 h with humidified methane at 700 °C, before the test was stopped with the cell still running well. Very little carbon was detected on the anodes, suggesting that carbon deposition was limited during cell operation.

Figs. 11 and 12 show secondary electron microscopic (SEM) images and carbon mapping images of the Ni/ScSZ anode and the 2.0 wt.%GDC-coated Ni/ScSZ anode, respectively, which was operated at 700 °C in humidified methane under open circuit condition for 73 and 84 h, respectively. Fig. 11(b), taken from a region near the Ni/ScSZ anode free surface, shows clear and strong carbon deposition, which suggests that coke builds

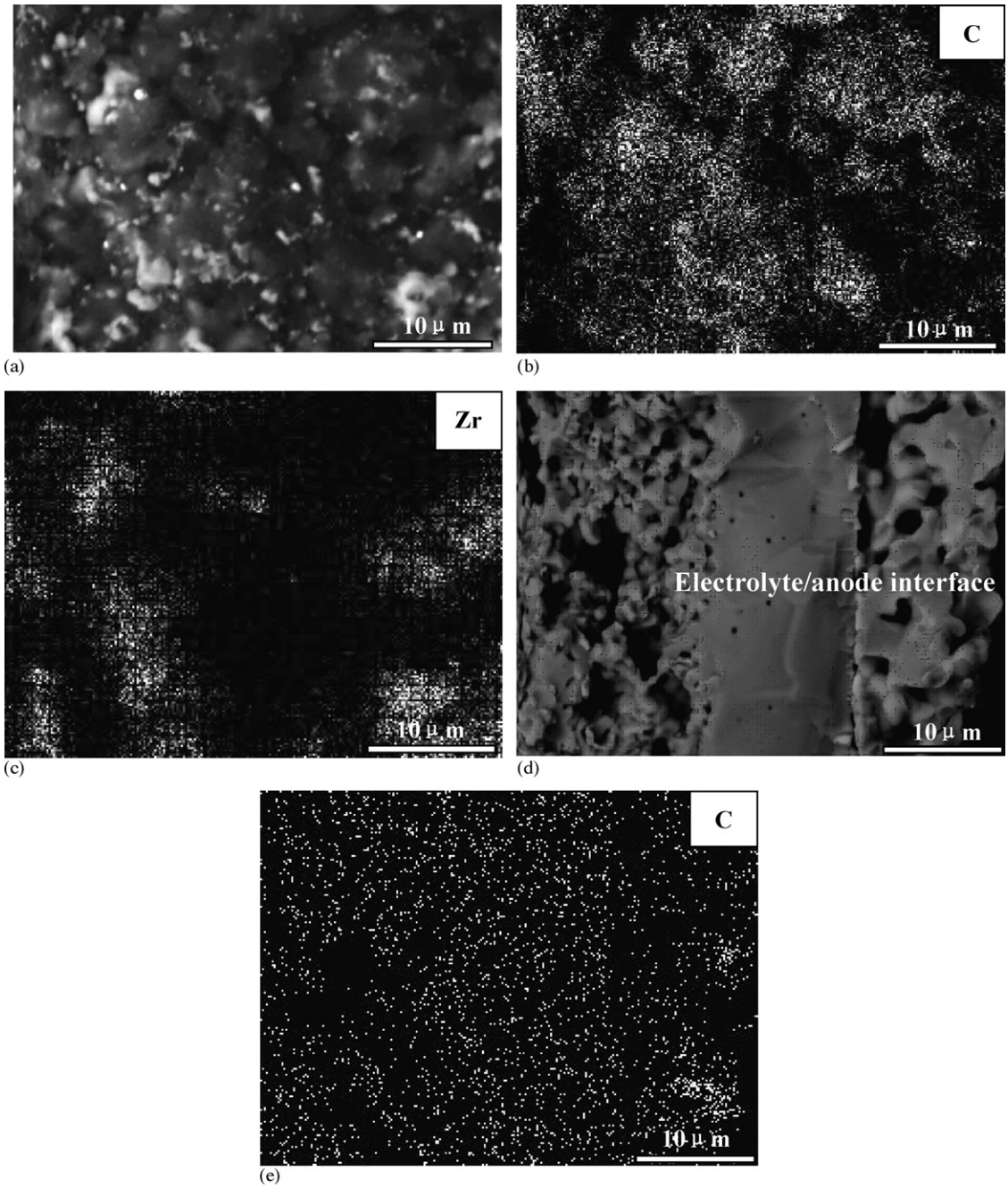

Fig. 11. Electron probe microscopic analysis (EPMA) of Ni/ScSZ anode operated in humidified methane at 700 °C under open circuit condition for 73 h: (a) SEM image of the anode free surface; (b) C mapping of the anode free surface; (c) Zr mapping of the anode free surface; (d) SEM image of anode/electrolyte interface; (e) C mapping of anode/electrolyte interface.

up within the anode; this may cause performance degradation shown in Fig. 10(a) by one or more mechanism. For example, carbon may block anode pores, degrading cell performance. Alternatively, the coke buildup may lead to volume expansion and consequent micro-cracking, presumably leading to an interruption of anode current collection pathways. Fig. 11(b) does not show any evidence of micro-cracking, performance degradation was often observed after long-term cell operation under coking conditions. Fig. 11(e) shows little carbon deposition in the region of the anode/electrolyte interfaces in contrast with the carbon mapping in the region near the anode free surface. These results showed that carbon deposition decreased from the free surface (Fig. 11(b)) towards the electrolyte. Fig. 12(b) taken from a region near the 2.0 wt.%GDC-coated Ni/ScSZ anode free surface, shows little carbon deposition compared to the Ni/ScSZ anode free surface. As can be seen from Fig. 12(f), there is no carbon deposition in the region of the anode/electrolyte interfaces in contrast with the carbon mapping in the region near the anode free surface (Fig. 12(b)). From these results, we find that the GDC coating can reduce carbon deposition in the anode.

However, much more work needs to be done to clarify the effect of the GDC coating on the catalytic activities for oxida-

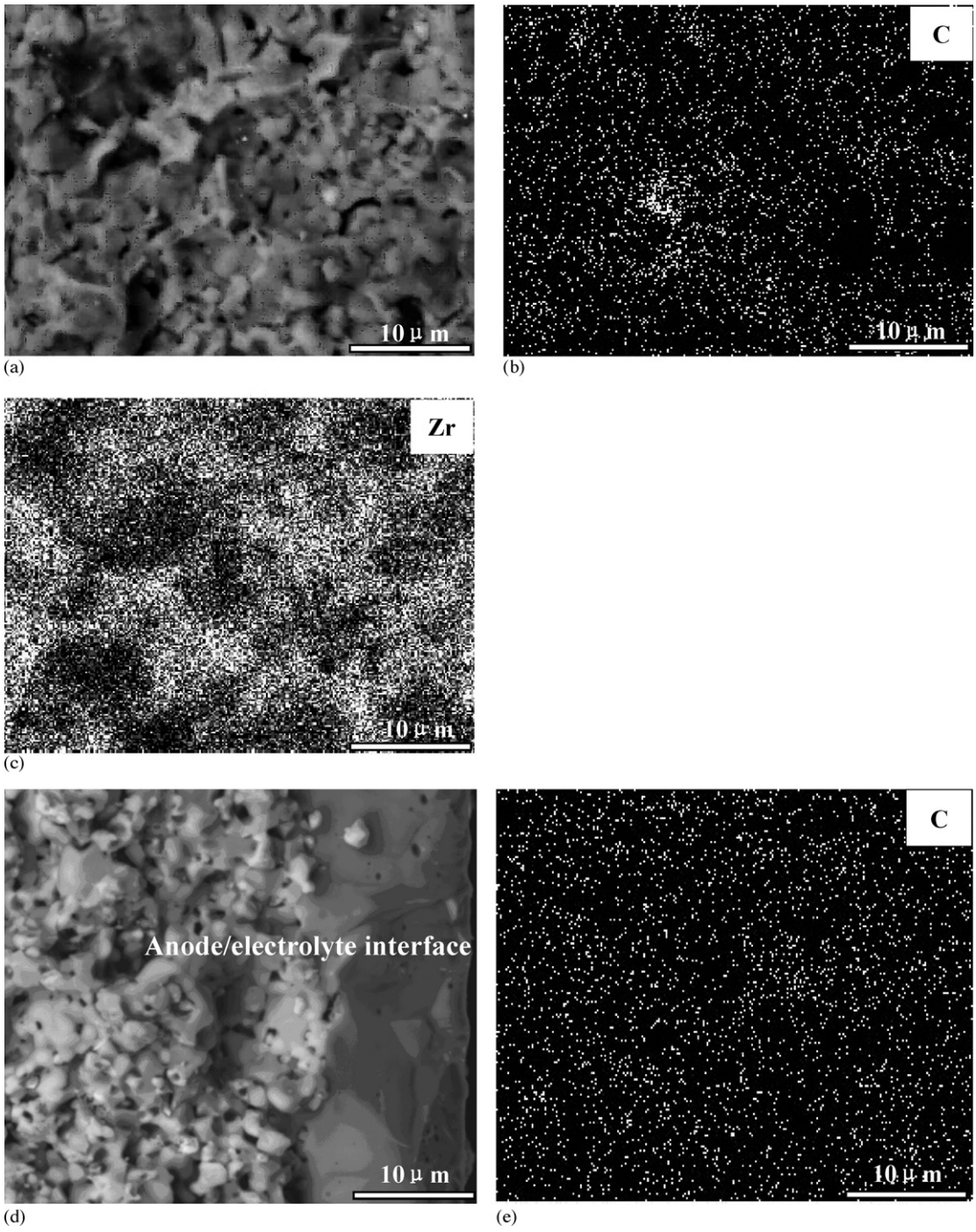

Fig. 12. Electron probe microscopic analysis (EPMA) of 2.0 wt.%GDC-coated Ni/ScSZ anode operated in humidified methane at 700 °C under open circuit condition for 84 h: (a) SEM image of the anode free surface; (b) C mapping of the anode free surface; (c) Zr mapping of the anode free surface; (d) SEM image of anode/electrolyte interface; (e) C mapping of anode/electrolyte interface.

tion of methane, determine the stability for long-term operation and clarify the effect of the loading of GDC coating on the electrochemical activity of Ni/ScSZ anode.

4. Conclusions

Nano-sized $Gd_{0.2}Ce_{0.8}O_2$ particles were coated within the pores of porous Ni/ScSZ anode using a simple combustion process. The present results show that anode supported SOFCs with 2.0 wt.%GDC-coated Ni/ScSZ anode can be operated directly with humidified methane, yielding high power densities. The measured OCV dependence on temperature was consistent with calculated values. The coating of nano-sized $Gd_{0.2}Ce_{0.8}O_2$ particle within the pores of the porous Ni/ScSZ anode significantly improved the performance of anode supported cells. Electrochemical impedance spectra illustrated that the cell with Ni/ScSZ anode exhibited far greater impedances than the cell with 2.0 wt.%GDC-coated Ni/ScSZ anode. Intro-

duction of nano-sized GDC particles into the pores of porous Ni/ScSZ anode will result in a substantial increase in the ionic conductivity of the anode and increase the triple phase boundary region expanding the number of sites available for electrochemical activity. Cell stability tests show that no significant degradation in performance has been observed after 84 h of cell testing when 2.0 wt.%GDC-coated Ni/ScSZ anode was exposed to 97%CH_4/3%H_2O at 700 °C. Very little carbon was detected on the anodes, suggesting that carbon deposition was limited during cell operation. Therefore, 2.0 wt.%GDC-coated Ni/ScSZ anode could be used as an alternative anode for an SOFC running on methane fuel. We made novel alternative anode material using coating of GDC within the pores of the Ni/ScSZ anode. Using the manufacturing method, we expect that economical and large-scale anode can be made easily.

Acknowledgements

The authors thank the Shanghai Institute of Ceramics Chinese Academy of Sciences and the Postdoctoral Foundation of Shanghai (Grant No. 2003003295) for the grants that support this research.

References

[1] T. Setoguchi, M. Sawano, K. Eguchi, H. Arai, Solid State Ionics 40–41 (1990) 502.
[2] J. Schoonman, J.P. Dekker, J.W. Broers, N.J. Kiwiet, Solid State Ionics 46 (1991) 299.
[3] V.E.J. van Dieten, J. Schoonman, Solid State Ionics 57 (1992) 141.
[4] C.C. Chen, M.M. Nasrallah, H.U. Anderson, Solid State Ionics 70–71 (1994) 101.
[5] T. Hibino, A. Hashimoto, K. Asano, M. Yano, M. Suzuki, M. Sano, Electrochem. Solid-State Lett. 5 (2002) A242.
[6] Z. Shao, S.M. Haile, Nature 431 (2004) 170.
[7] B.C.H. Steel, Nature 400 (1999) 619.
[8] C. Lu, W.L. Worrell, C. Wang, S. Park, H. Kim, J.M. Vohs, R.J. Gorte, Solid State Ionics 152–153 (2002) 393.
[9] J. Liu, S.A. Barnett, Solid State Ionics 158 (2003) 11.
[10] J.-H. Koh, Y.-S. Yoo, J.-W. Park, H.C. Lim, Solid State Ionics 149 (2002) 157.
[11] J.B. Wang, J.-C. Jang, T.-J. Huang, J. Power Sources 122 (2003) 122.
[12] C.H. Bartholomew, Catal. Rev. Sci. Eng. 24 (1982) 67.
[13] R.T.K. Baker, Carbon 27 (1989) 315.
[14] B.C.H. Steele, Solid State Ionics 86–88 (1996) 1223.
[15] K. Hernadi, A. Fonseca, J.B. Nagy, A. Siska, I. Kiricsi, Appl. Catal. A 199 (2000) 245.
[16] J.H. Koh, Y.-S. Yoo, J.-W. Park, H.C. Lim, Solid State Ionics 149 (2002) 157.
[17] T. Tsai, S.A. Barnett, J. Electrochem. Soc. 142 (1995) 3084.
[18] S. de Souza, S.J. Visco, L.C. De Jonghe, J. Electrochem. Soc. 144 (1997) L35.
[19] P. Muccillo, E.N.S. Muccillo, F.C. Fonseca, Y.V. Franca, T.C. Porfirio, D.Z. de Florio, M.A.C. Berton, C.M. Garcia, J. Power Sources 156 (2006) 455–460.
[20] S.P. Yoon, J. Han, S.W. Nam, T.-H. Lim, S.-A. Hong, J. Power Sources 136 (2004) 30–36.
[21] C.E. Hori, H. Permana, K.Y. Simon Ng, A. Brenner, K. More, K.M. Rahmoeller, D. Belton, Appl. Catal. B 16 (1998) 105–117.
[22] R. Morrel, Handbook of Properties, Technical and Engineering Ceramic, Part 1, NPL, 1986.
[23] S. Jain, K. Adiga, V. Vrneker, Combust. Flame 40 (1981) 71.
[24] R. Zheng, X.M. Zhou, S.R. Wang, T.-L. Wen, C.X. Ding, J. Power Sources 140 (2005) 217–225.
[25] S. de Souza, S.J. Visco, L.C. De Jonghe, J. Electrochem. Soc. 144 (1997) L35.
[26] J.W. Kim, A.V. Virkar, K.Z. Fung, K. Mehta, S.C. Singhal, J. Electrochem. Soc. 146 (1) (1999) 69–78.
[27] R. Farrauto, M. Hobson, T. Kennelly, E. Waterman, Appl. Catal. A81 (1992) 227.
[28] J. Liu, S.A. Barnett, Solid State Ionics 158 (2003) 11–16.
[29] M. Godickemeier, K. Sasaki, L.J. Gauckler, in: M. Dokiya, O. Yamamoto, H. Tagawa, S.C. Singhal (Eds.), Proceedings of the 4th International Symposium on Solid Oxide Fuel Cell, Electrochemical Society, Pennington, 1995, pp. 1072–1081.
[30] C.E. Hori, et al., Appl. Catal. B 16 (1998) 105–117.
[31] H. Kim, C. Lu, W.L. Worrell, J.M. Vohs, R.J. Gorte, J. Electrochem. Soc. 149 (3) (2002) A247–A250.